

group (140 [100–180] μm to 160 [125–205] μm ; $p < 0.01$), whereas the FCT did not change in the late statin group (120 [100–150] μm to 120 [100–150] μm , $p = 0.29$). Percent change in the FCT was significantly greater in the early statin group (110 [92–137] % vs. 98 [85–110] %, $p < 0.01$). The percent change in the FCT was negatively correlated with percent change in serum malondialdehyde-modified low-density lipoprotein levels ($r = -0.43$, $p < 0.01$). During 6-month follow-up the FCT increased in both groups, and percent change in the FCT between baseline and 6-month follow-up was comparable between the 2 groups.

Conclusion: Increase of FCT in coronary plaque was observed at 3 weeks after starting statin therapy, and a further increase was obtained at 6-month follow-up. Statin might have an early beneficial plaque-stabilizing effects in patients with ACS.

3083 | BEDSIDE
Epicardial fatty tissue derived by cardiac magnetic resonance imaging is related to coronary plaque vulnerability as assessed by optical coherence tomography in patients with type 2 diabetes

D. Zhu, S. Reith, N. Marx, M. Burgmaier. RWTH University Hospital Aachen, Internal Medicine I, Cardiology, Aachen, Germany

Background: Patients with type 2 diabetes are at an increased risk for vulnerable coronary plaques and subsequent cardiovascular events. Given that patients with type 2 diabetes have more epicardial fatty tissue (EFT) compared to patients without diabetes and as EFT may be involved in the pathogenesis of coronary artery disease (CAD), we hypothesized that there may be a relationship between EFT and features of coronary plaque vulnerability in patients with type 2 diabetes.

Methods: Optical coherence tomography (OCT) was performed in the coronary culprit lesion of 58 patients with type 2 diabetes and stable CAD in order to assess plaque composition including morphologic features of plaque vulnerability. Furthermore, EFT was quantified using cardiac magnetic resonance imaging (cMRI) as described previously.

Results: The mean fibrous cap thickness (mean FCT) overlying the necrotic lipid core of the target lesions was $128 \pm 30 \mu\text{m}$. EFT was related to mean FCT of the target lesions on linear regression analysis ($r = 0.375$, $p = 0.01$). Furthermore, EFT predicted a thinner mean FCT ($< 128 \mu\text{m}$) on univariable logistic regression analysis (OR 3.956, 95% confidence interval (CI) 1.331–11.760, $p = 0.013$). Multivariable logistic regression analysis using adjustments for 1. body mass index and waist circumference (OR 4.822, 95% CI 1.305–17.823, $p = 0.022$) and 2. additional adjustments for mean arterial pressure and HbA1C (OR 4.065, 95% CI 1.056–15.641, $p = 0.041$) demonstrated that EFT is an independent predictor for a thin mean FCT.

Conclusion: CMRI-derived EFT is related to the mean FCT as assessed by OCT in coronary culprit lesions of patients with type 2 diabetes and stable CAD. Future studies are warranted to evaluate if there is a causal role between EFT and features of coronary plaque vulnerability in patients with type 2 diabetes.

COMPUTER MODELLING AND SIMULATION

P3084 | BENCH
A validated computational framework to simulate transcatheter aortic valve implantation in patients before the procedure

G.M. Bosi¹, C. Capelli¹, M.H. Cheang², N. Delahunty², M. Mullen², A.M. Taylor³, S. Schievano¹. ¹University College London, Institute of Cardiovascular Science, London, United Kingdom; ²Barts Health NHS Trust, London, United Kingdom; ³Great Ormond Street Hospital for Children, Centre for Cardiovascular Imaging, London, United Kingdom

Introduction: Second generation of existing transcatheter aortic valve implantation (TAVI) technologies, along with a host of new devices, are being developed to overcome the remaining issues associated with first generation TAVI devices, including valve malpositioning, vascular complications, paravalvular regurgitation (PVR) and conduction disorders. Indications for TAVI are also evolving, widening the number of patients who can benefit from this minimally invasive procedure. In this context, computational simulations, already an established tool to support engineering device development, could be useful, with a patient-specific approach, to introduce new technologies in clinical practice.

Purpose: The aim of this work was to develop and validate a patient-specific computational framework for prediction of TAVI outcomes, that could be used to test new devices in realistic implantation sites and to enhance patient safety in the early introduction of new technologies in clinics. The implantation site computational model was validated using retrospective cases treated with first generation devices.

Methods: Twenty eight patients who underwent TAVI with balloon-expandable (BE) ($n = 14$) and with self-expandable (SE) ($n = 14$) devices were retrospectively selected. Pre-procedural computed tomography images were post-processed to create the 3D patient-specific anatomy of the implantation site, including outflow tract, root, ascending aorta, leaflets, coronary arteries and calcifications. Material properties were selected from literature and optimised for TAVI patients. Post-procedural fluoroscopy and echocardiography images were analysed to assess diameters of the implanted TAVI device, and onset and position of PVR. Balloon valvuloplasty and device deployment were simulated. An automatic code was implemented to assess the simulation results: diameters, device/implantation site

contact, presence and location of PVR (Fig. 1a), stress on the cardiac conduction system below the coronary ostia for comparison with conduction complications reported for the patient population.

Results: The comparison between stent diameters measured from fluoroscopy images and computational results showed a mean difference of -1.04% (max 9.9%) for BE and -0.06% (max -7.1%) for SE implantations. Presence of PVR was identified by the automatic code in 93% of BE and 85% of SE cases, while correct location in 93% and 75% of cases respectively. The sole patient who developed conduction abnormalities (Fig. 1b), from the SE cohort, showed the highest stress distribution, thus providing a potential computational parameter to monitor this risk.

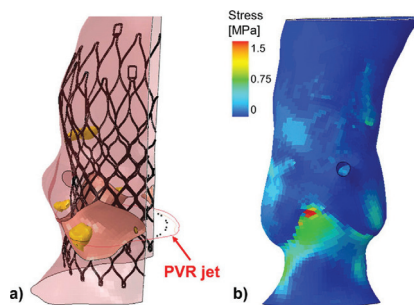


Figure 1

Conclusion: The developed and validated patient-specific computational framework could be used on one side to aid the design and test of new TAVI devices in virtual implantation sites with realistic geometries and materials, and, on the other, to enhance the assessment of patients selected for the implantation of new devices.

Acknowledgement/Funding: GM Bosi was funded by the British Heart Foundation (FS/13/11/30056).

P3085 | BENCH
Cerebral hypoperfusions and hypertensive events during atrial fibrillation: a mechanism for cognitive impairment?

M. Anselmino¹, A. Saglietto¹, S. Scarsoglio², L. Ridolfi³, F. Gaita¹. ¹Hospital "Città della Salute e della Scienza di Torino", Division of Cardiology, Department of Medical Sciences, Turin, Italy; ²Politecnico di Torino, Department of Mechanical and Aerospace Engineering, Turin, Italy; ³Politecnico di Torino, Department of Environmental, Land and Infrastructure Engineering, Turin, Italy

Background: Atrial fibrillation (AF) is associated with an increased risk of dementia and cognitive decline, independent of clinical strokes/TIAs. Several mechanisms have been proposed to explain this association, but altered cerebral blood flow dynamics during AF has been poorly investigated: in particular, it is unknown how AF influences hemodynamic parameters of the deepest cerebral circulation.

Purpose: Aim of the present study was to study AF impact on cerebral circulation through a computational hemodynamic analysis.

Methods: Two coupled lumped-parameter models (systemic and cerebrovascular circulations, respectively) were used to simulate sinus rhythm (SR) and AF.

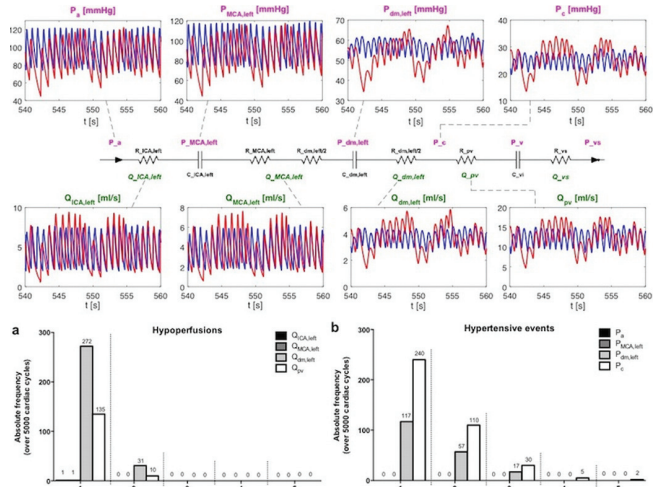


Figure 1. Top panel: representative pressure and flow rate time series are reported for the internal carotid artery-middle cerebral artery (ICA-MCA) pathway during SR (blue) and AF (red). Lower panel: absolute frequency of hypoperfusions (a) and hypertensive events (b) during AF along the ICA-MCA pathway; the abscissa indicates the number of consecutive beats characterizing the events. P(a): systemic arterial pressure; P(MCA,left): left middle cerebral artery pressure; P(dm,left): left middle distal pressure; P(c): cerebral capillary pressure; Q(ICA,left): left internal carotid flow rate; Q(MCA,left): left middle cerebral artery flow rate; Q(dm,left): left middle distal flow rate; Q(pv): proximal venous flow rate.

For each simulation 5,000 cardiac cycles were analyzed, computing main statistics (mean and standard deviation) for different cerebral hemodynamic parameters.

Results: With respect to SR, AF triggered a greater variability (represented by the standard deviation) of the parameters, especially in the deepest circulation (cerebral arterioles and capillaries; see Figure, top panel). This variability led to critical cerebral hemodynamic events: during AF 303 hypoperfusions (maximum duration: 2 beats) occurred at the arteriolar level, while 387 hypertensive events (maximum duration: 5 beats) occurred at the capillary level (see Figure, lower panel). By contrast, neither hypoperfusions nor hypertensive events occurred during SR.

Conclusion: During AF, the higher variability of the cerebral hemodynamic variables increases proceeding towards the peripheral circulation, reaching the maximum extent at the arteriolar and capillary levels and possibly resulting in local transient periods of excessive pressure or reduced blood flow. Thus, the impact of AF per se on cerebral hemodynamics candidates as a relevant mechanism into the genesis of AF-related cognitive impairment/dementia.

P3086 | BEDSIDE

Can computational fluid dynamics (CFD) predictions of FFR really agree with invasive FFR in intermediate stenoses? Lessons from a study using optical coherence tomography (OCT) and invasive measures

C.M. Cook, C. Kouser, Y. Ahmad, R. Petraco, S. Nijjer, R. Al-Lamee, A. Sethi, D. Francis, S. Sen, J.E. Davies. *Imperial College London, NHLI, International Centre for Circulatory Health, London, United Kingdom*

Background: Computational fluid dynamics (CFD) modelling can estimate lesion specific FFR values (FFRCFD) from computed tomography coronary angiography (CCTA) images. The upper limit of accuracy of this technique may therefore be limited by i) the luminal characterisation ability of CCTA; and ii) the reliance of CFD on estimated boundary conditions of coronary flow and pressure.

Purpose: To assess the upper limits of agreement between FFRCFD and invasive FFR in intermediate coronary stenoses, using gold standard luminal imaging with optical coherence tomography (OCT) and invasively measured (i.e. patient specific) boundary conditions of resting and hyperaemic flow.

Methods: 19 patients (21 vessels) with angiographically intermediate stenoses were included for study. 3D geometric reconstructions of 21 coronary artery lumens were made using co-registered biplane angiography views and optical coherence tomography (OCT) images. Simultaneous pressure and Doppler flow velocity measurements defined patient specific boundary conditions for the CFD model. CFD simulations with very high spatial resolution (120,000–150,000 tiny cubes and prisms per vessel) were performed in commercial software Ansys CFX 13.0 (ANSYS UK) and FFRCFD compared to invasively measured FFR. A sensitivity analysis of the CFD simulations to varying flow rate levels within the physiological range during hyperaemia (1.2 to 2.8 ml/s) was performed across a range of stenosis severities. Overall diagnostic performance of FFRCFD was assessed with invasive FFR as the reference standard.

Results: 19 patients (age 65.9±10.8; 14 (73.7) male) with 21 stenoses (LAD = 13, RCA = 5, LCx = 3) and a mean area stenosis of 66% (±12) were included for study. Mean, median and IQR values for FFR and FFRCFD were 0.85 (±0.07), 0.85, 0.11 and 0.86 (±0.08), 0.88, 0.10 respectively. On a per-vessel basis, accuracy, sensitivity, specificity, positive predictive value, and negative predictive

values were 71.4%, 33.3%, 86.7%, 50.0%, 76.5%, respectively, for FFRCFD with gold standard luminal imaging and patient specific boundary conditions of resting and hyperaemic coronary flow. Pearson's correlation coefficient of per-vessel FFRCFD values with FFR values was 0.57 ($p=0.007$). In the sensitivity analysis of the CFD simulations to varying volumetric flow rate levels, an increase of flow rate by 1ml/s decreased FFRCFD value by 0.40, 0.35 and 0.20 in severe, intermediate and mild stenoses respectively.

Conclusions: In intermediate stenoses, using close to exact conditions for CFD (gold standard luminal imaging and patient specific boundary conditions), the diagnostic accuracy of FFRCFD was 71.4%. A major limitation of the concept of CFD is the requirement to estimate hyperaemic volumetric flow rate as a boundary condition. In this study, changes within the physiological range for hyperaemic flow conditions altered FFRCFD values by as much as 40%.

Acknowledgement/Funding: Medical Research Council Fellowship Grant (Dr Cook)

P3087 | BENCH

Study of the impact of electrical heterogeneities in the right and left atrium on atrial fibrillation perpetuation

A. Luca¹, V. Jacquemet², N. Virag³, J.-M. Vesin¹. ¹Swiss Federal Institute of Technology, Lausanne, Switzerland; ²Hospital du Sacre-Coeur, Montreal, Canada; ³Medtronic Europe, Tolochenaz, Switzerland

Introduction: Electrical heterogeneity in the atria has been consistently linked with the initiation and perpetuation of atrial fibrillation (AF). The present model-based study investigated the contribution of action potential duration (APD) heterogeneities in the left atrium (LA) and right atrium (RA) on the perpetuation of the reentrant activity during AF.

Methods: A computer model with a geometry based on computed tomography of AF patients and a Courtemanche atrial cellular model was implemented. Self-terminated AF episodes were initiated via ramp pacing in a model with modified channel conductance, homogeneous tissue and 4:1 anisotropy ratio. Once AF was observed, random patchy heterogeneities with shorter APD were separately introduced in the LA and the RA. Percentage of heterogeneities was progressively increased from 20% to 80% of each atrium size (characteristic length scale of patches was 7.5mm). For each simulation, the following values were assessed: average AF duration, the number of sustained AF episodes (lasting more than 50s), number of wave-fronts (#WF) and AF cycle length (AFCL). The results were averaged across the atria surface over 130 simulations (26 AF initial conditions and 5 random localizations of heterogeneities).

Results: For the model with no heterogeneities, #WF was 6.82±3.67, AFCL 278±52ms and the average AF duration 15.42±9s. For low percentage of heterogeneities there were no significant differences between RA, LA and the model with no heterogeneities. For high percentage of heterogeneities the results showed that a significant right-to-left atrial APD gradient was associated with more sustained AF episodes, longer duration, higher #WF and shorter AFCL compared to the left-to-right APD gradient (sustained AF episodes: 95% vs. 52%, $p<10^{-4}$; duration: 48±9s vs. 32.8±21s, $p<0.05$; #WF: 11.72±3.3 vs. 9.7±3.1, $p<10^{-4}$; AFCL: 209±69ms vs. 223±64ms, $p<0.05$).

Conclusion: High inter-atria differences in APD significantly affect the dynamics and the duration of the reentrant activity. Our findings are in line with previous studies reporting the right atrium as the dominant driver in some persistent AF cases.

Acknowledgement/Funding: This study was supported by the TRM Foundation.

P3088 | BEDSIDE

Systematic review of non-invasive computed tomography-derived FFR (FFR-CT) studies to guide integration of FFR-CT into mainstream clinical practice

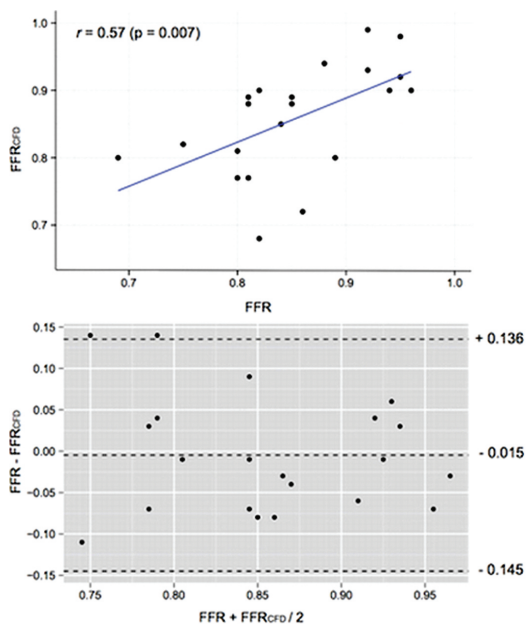
C.M. Cook, R. Petraco, Y. Ahmad, S. Nijjer, R. Al-Lamee, M. Shun-Shin, Y. Shiono, Y. Kikuta, D. Francis, S. Sen, J.E. Davies. *Imperial College London, NHLI, International Centre for Circulatory Health, London, United Kingdom*

Background: How to optimally integrate FFR-CT into clinical practice is not known. Overall diagnostic accuracy values provide only an overview across entire ranges of disease severity, in study populations that can differ from clinical cohorts. To interpret FFR-CT values on a patient-by-patient basis, diagnostic accuracy needs to be evaluated across narrow ranges of disease severity, in a sample-independent manner.

Purpose: To formulate a strategy for integrating non-invasive computed tomography-derived FFR (FFR-CT) into mainstream clinical practice

Methods: A systematic review was performed of all studies that i) quantified physiological stenosis severity with both FFR-CT and invasive FFR (blinded); and ii) displayed a scatter plot of FFR-CT and invasive FFR values. Data were digitized to extract the individual data points for analyses of diagnostic performance. A per-quantile analysis of FFR-CT diagnostic accuracy was performed in each 0.10 FFR-CT disease quantile from 0.20 to 1.00. FFR-CT ≤ 0.80 and FFR ≤ 0.80 was used as the diagnostic cut-point, with invasive FFR as the reference standard.

Results: 4 studies (422 vessels) met the inclusion criteria. Mean age was 62.9 years (72% male). The overall diagnostic accuracy of FFR-CT was 77.5%, however, at the extremes of disease severity, FFR-CT values >0.90 and <0.50 demonstrated 93% and 85% agreement with invasive FFR respectively. Con-



OCT derived FFR-CFD vs FFR